Lawrence Berkeley Laboratory
UNIVERSITY OF CALIFORNIA

Materials & Molecular
Research Division

Submitted to Scripta Metallurgica

CARBON ATOM DISTRIBUTION IN A DUAL PHASE STEEL: AN ATOM PROBE STUDY

S.J. Barnard, G.D.W. Smith, M. Sarikaya, and G. Thomas

January 1981

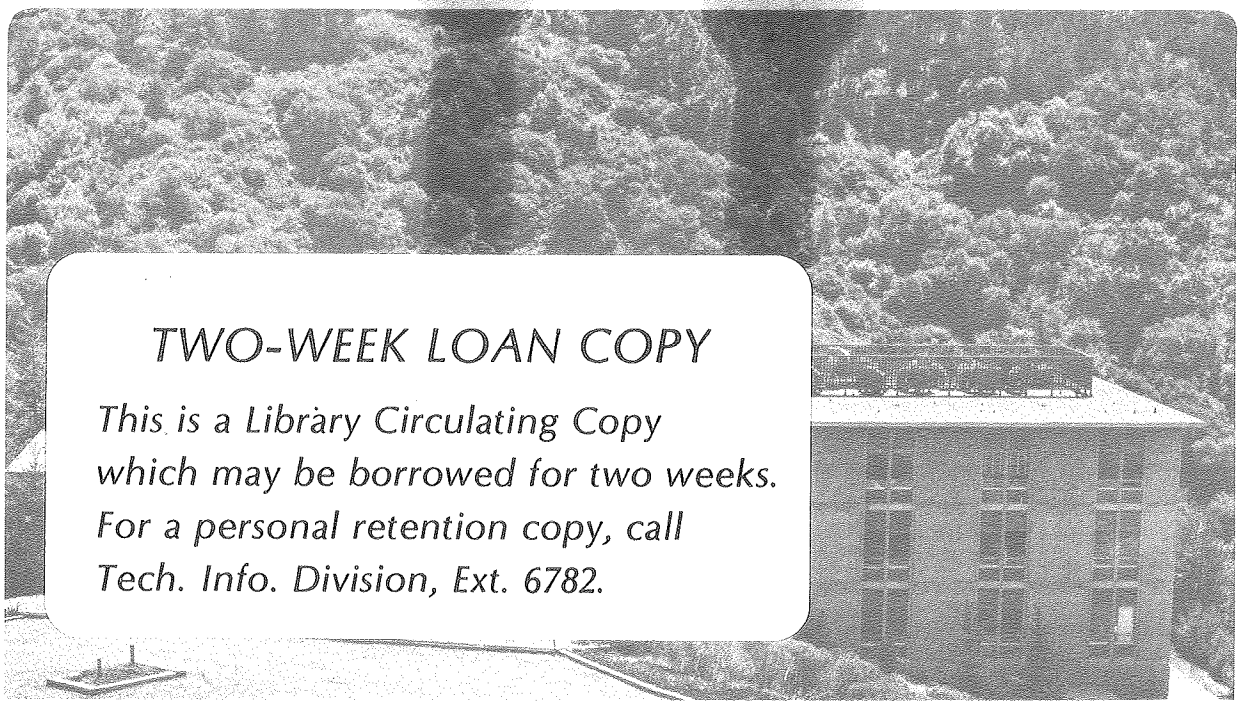

Prepared for the U.S. Department of Energy under Contract W-7405-ENG-48

DISCLAIMER

CARBON ATOM DISTRIBUTION IN A DUAL PHASE STEEL: AN ATOM PROBE STUDY

S.J. Barnard and G.D.W. Smith
Department of Metallurgy and Science of Materials, University of Oxford,
Parks Road, Oxford, England

and

M. Sarikaya and G. Thomas
Department of Materials Science and Mineral Engineering,
Lawrence Berkeley Laboratory,
University of California, Berkeley, California 94720, U.S.A.

Introduction

Dual Phase steels are currently attracting considerable attention because of their outstanding mechanical properties (1). Compared with other commercially-available steels of equivalent carbon content, the martensite-austenite form shows superior toughness and ductility and the martensite-ferrite form has improved tensile strength whilst maintaining good formability. This paper is concerned in particular with the mechanism of stabilisation of the austenite phase in a martensite-austenite dual phase steel, although the results are of general applicability to any system where austenite is retained in a martensite matrix.

Austenite is found to be stabilised under a number of circumstances, indicating that several mechanisms probably contribute to overall stability. In this work, we investigate the role of carbon in the transformation process, using a computer-controlled atom probe field ion microscope system (2,3) to directly and quantitatively measure the carbon distribution at the atomic level. Previous efforts to determine carbon atom distributions in these steels by other experimental techniques have encountered a number of difficulties. X-ray microanalytical methods lack sensitivity to carbon, and attempts to use electron energy loss techniques have also so far been unsuccessful. Accurate X-ray diffraction lattice parameter measurements are not possible, because of the very fine scale of the distribution of the retained austenite in the form of thin films between the martensite laths. The only experimental approach which has permitted an estimate to be made of the carbon content of the austenite phase is that of lattice imaging (4,5, 6). Considerable difficulties are associated with this technique, since electron optical phenomena are known to affect lattice fringe spacings, the most important parameters being specimen thickness and deviation (s) from the exact Bragg condition (6). In certain favourable cases it has proved possible to obtain lattice images from the martensite and austenite phases simultaneously, thus enabling the martensite fringe spacing to be used as a calibration for the austenite (5). However, this requires an assumption to be made regarding the carbon level in the martensite phase, which is usually taken to be the nominal value for the steel concerned. Despite these limitations, the lattice imaging technique has produced indications of a substantial enrichment in carbon level in the austenite phase. The object of the present work is to obtain an independent measurement of the carbon content of each phase, and also to investigate the segregation of carbon to interfaces and other lattice defects such as dislocations.

Experimental

A single alloy was used for this initial investigation. The composition and heat treatments are given below.

Element	C	Cr	Mn	Ni	Mo	Si	Fe
wt%	0.26	2.99	1.98	0.01	0.50	0.07	bal.
at%	1.20	3.18	1.99	0.01	0.29	0.14	bal.

The M_s temperature for this steel is approximately 320°C, and M_f about 260°C.

This work was partially supported by the U.K. Science Research Council, and partially supported by the Director, Office of Energy Research, Office of Basic Energy Sciences, Division of Materials Sciences of the U.S. Department of Energy under Contract No. W-7405-ENG-48.

extremely rarely (for example none was found in an analysis of 7,500 ions taken from the martensite phase). If a C-Mo complex ion is formed, it can only be to a very small extent, since the nominal level of molybdenum can be accounted for in the +1 and +2 charge states.

The results of quantitative analyses of carbon levels in the martensite and austenite phases of a number of specimens are summarised in Table I below.

TABLE I
Analyses of Carbon Concentrations in Martensite and Austenite Phases

	Atomic Concentration %	No.of ions in spectrum	Heat treatment
Martensite	0.06 ± 0.06	1,612	I
	0.17 ± 0.05	7,495	I
	0.07 ± 0.04	4,200	II
	0.16 ± 0.05	7,001	II
Austenite	2.24 ± 0.25	3,435	I
	2.25 ± 0.37	1,600	II
	2.27 ± 0.39	1,500	II
	2.64 ± 0.48	1,100	II

It can be seen that the results obtained from the two heat treatments are essentially the same. In each case, the carbon level in the austenite phase is enriched by a factor of about 2 with respect to the nominal level in the steel. In the martensite phase, on the other hand, the level of carbon in the matrix is extremely low. In part this must be due to the precipitation of fine carbides during the final tempering treatment at 200°C (e.g. Fig 3). However, two additional effects can be identified. Firstly, a particularly high concentration of carbon is observed at the martensite-austenite interface. Fig 6 shows a typical distribution of carbon in the region of such an interface. The cumulative total number of ions caught, which is plotted as the abscissa of this graph, may be taken as a measure of distance evaporated through the specimen; 100 ions is roughly equivalent to 0.4nm. In a series of such traverses across martensite-austenite interfaces, the peak concentrations of carbon measured were in the range 10-24% (averaged over 100 ions). Since the effective aperture for data collection was about 2nm diameter in each case, it is possible that the carbon content in the actual plane of the interface is even higher than the range of values given above.

The second additional effect identified concerns the fine-scale distribution of carbon within the martensite laths. It appears that this distribution is markedly inhomogeneous. In addition to the very low background levels quoted in Table I, small localised regions are found, apparently remote from the fine carbides, in which the carbon concentration rises to the level of a few per cent over the distance of one or two nanometres. It seems likely that these local concentrations arise from the clustering of carbon atoms in the region of dislocations. Further work is in progress to substantiate this point.

Discussion

The most salient features of the experimental results described above are as follows:
(i) a substantial enrichment of carbon in the retained austenite films.
(ii) a large peak in carbon concentration at the martensite-austenite austenite interface.
(iii) a marked inhomogeneity in the distribution of carbon in the martensite phase.

These effects will be discussed in turn.

The observation of carbon enrichment in the retained austenite films provides direct evidence of the chemical stabilisation of this phase. In general terms, the quantitative analyses produced by the atom probe are in agreement with the previous indirect measurements of austenite carbon content based on lattice imaging methods (5). As mentioned earlier in this paper, the lattice fringe spacing measurements relied on using the martensite fringes as a calibration, and assumed that the carbon content of the martensite matrix was the same as the nominal content for the steel as a whole. It is therefore not altogether surprising that there is a spread in the lattice imaging results, depending on which set of martensite lattice fringes was used for calibration purposes. The atom probe data should permit an approximate correction to be made to the lattice fringe calculations, and this should enable a better comparison between the two techniques. This work is to be continued, and extended to as-quenched specimens.

Heat treatment I: Austenitise 1h at 1100°C, oil quench, re-austenitise 1h at 900°C, oil quench, temper 2h at 200°C, water quench.

Heat treatment II: As for I, but with an intermediate tempering between the two austenitisation treatments.

The microstructures obtained consisted of laths of martensite surrounded by thin films of retained austenite, the austenite volume fraction being a few per cent. Transmission electron microscopy has shown the tempered martensite to be heavily dislocated, and to contain a fine dispersion of carbides (5).

Heat treatment II gave a significantly finer microstructure than heat treatment I, but the results obtained for carbon atom distributions are essentially similar in each case.

Field ion specimens were prepared from 0.5mm square bars of the heat treated material using a two-stage polishing technique. The first stage consisted of a standard double layer polish with an electrolyte of 25% perchloric acid in acetic acid floated on carbon tetrachloride. This served to produce a neck in the centre of the bar. The second stage consisted of a single electrolyte of 2% perchloric acid in 2-butoxy-ethanol. This latter part of the polishing was continued briefly after the lower half of the bar had separated from the upper in order to remove any deformed layers from the specimen. Both stages of polishing were carried out at 25V D.C., and all solutions were initially cooled to 0°C.

The atom probe used in this investigation was a conventional time-of-flight instrument using a 159.6MHz digital timer, interfaced to a PDP 11/10 computer. A full description of the instrument can be found elsewhere (7). All analyses were carried out under the following experimental conditions:

a) a system base pressure of $<5 \times 10^{-10}$ torr
b) a background pressure during analysis of $<1 \times 10^{-9}$ torr i.e. with the image gas removed
c) the specimen cryostat cooled with liquid nitrogen
d) an effective data collection aperture of 2nm
e) a pulse fraction of 15%
f) a pulse repetition rate of 50Hz
g) ion collection rates of between 10^{-2} and 10^{-1} ions per pulse
h) a neon image gas pressure of 4×10^{-5} torr.

The data collected from the Atom Probe is sequential and hence both average analyses of each phase and variations of composition with distance are obtained. A more detailed explanation of data handling is given in reference (7).

Results

A series of field ion micrographs of the microstructures are shown in Figs 1-3. Fig 1 shows a specimen of heat treatment II, in which a thin, darkly imaging, band of retained austenite (arrowed) separates two martensite laths. Fig 2 shows the same specimen, later in the field evaporation sequence, when the dark austenite band is nearer to the centre of the image. The apparent curvature of the austenite is due to the planar film of the austenite layer intersecting the curved specimen surface at an oblique angle. Figure 3 shows a specimen of heat treatment I . In this case, the imaged region is fully martensitic, but a small carbide can be seen at the top right hand corner of the micrograph, near the martensite (200) pole. In all three micrographs, spiral configurations can be seen in the vicinity of major crystallographic poles in the martensite phase. These represent the points of emergence of dislocations at the surface of the specimens.

Typical atom probe spectra of the martensite and austenite phases are shown in Figs 4 and 5. The spectra are plotted on a semi-logarithmic scale to emphasise the minor peaks due to C, Cr, Mn, Si, and Mo. The carbon spectrum is particularly complex, with peaks at mass-to-charge ratios (m/n) 6, 12, 18, 24, and 36, due respectively to the species C^{++}, C^{+} or C_2^{++}, C_3^{++}, C_2^{+}, and C_3^{+}. It should be noted that the presence of molybdenum somewhat complicates the evaluation of the carbon concentration. The Mo +4 and +5 states have (m/n) values around 24 and 18 which overlap with the C_2^{+} and C_3^{++} peaks respectively. Also, there is a possibility that carbon and molybdenum could be associated in solid solution. If this were the case, then a C-Mo complex ion could possibly be produced, the (m/n) value for which in the triply charged state would be around 36, thus overlapping with the C_3^{+} peak. However, in practice it is found that the molybdenum charge states which would give rise to these ambiguities occur

The extent of the chemical stabilisation produced in the retained austenite by the increase in carbon content from the nominal level of 1.20 at% to the observed level of about 2.25 at% can be estimated from standard equations for the variation of M_s temperature with composition. The predicted decrease in M_s is of the order of 110°C. Since the M_s temperature of the steel is about 320°C, it is clear that chemical stabilisation alone is insufficient to account for the presence of retained austenite at room temperature. It is necessary to invoke additional mechanisms, such as mechanical stabilisation, to account for the exceptional stability of the austenite films in these steels.

The large peak in carbon concentration at the martensite-austenite interface is also of considerable interest. It is well known that holding a martensitic steel at a temperature intermediate between M_s and M_f leads to thermal stabilisation of the austenite. Low temperature tempering of such a partially-transformed structure leads to a substantial enhancement of the stabilisation process (8). The present observation of a very large local concentration of carbon at the transformation interface in such a tempered steel provides a simple and direct explanation for the retardation of subsequent reaction.

These results also help to explain the observed interlath decomposition on tempering of austenite to cementite (Temper Martensite Embrittlement) (9) in alloys containing retained austenite after quenching. Furthermore, the present data confirm the question as to whether lath martensite is really martensite or better referred to as "untransformed upper bainite" (5), since considerable diffusion must occur to account for the high carbon levels in the untransformed austenite.

The observation of inhomogeneous distribution of carbon within the martensite phase is strongly indicative of the segregation of carbon to lattice defects such as dislocations. However, the visibility or otherwise of a dislocation in the FIM

image depends on the orientation of its Burgers vector with respect to the local surface normal. Also, a dislocation may be pulled away from its solute atmosphere during FIM imaging, due to the mechanical stress associated with the imaging electric field. Thus a simple one-to-one correlation between solute enriched regions in the specimen and the observation of dislocation spirals in the image would not be expected and indeed is not found. Further careful work will be required to establish in detail the nature of these solute atmospheres. Finally, the possible relationship between the present measurements of carbon atom distribution and the mechanical properties of dual phase steels should be mentioned. It is clear that the properties of these steels must depend both on the chemical composition of each phase present, and on its stability. The present work opens up the possibility of new areas of study in the field of structure-property correlations. It is planned to continue the work with a series of alloys, to study the effects of different heat treatments upon carbon distributions, and to relate these to existing mechanical property measurements.

Acknowledgements

SJB and GDWS acknowledge the provision of financial support from the U.K. Science Research Council, and the provision of laboratory facilities by Professor Sir Peter Hirsch, FRS. MS and GT acknowledge support from the Director, Office of Energy Research, Office of Basic Energy Sciences, Division of Materials Sciences of the U.S. Department of Energy under Contract No. W-7405-ENG-48. Additionally, they wish to thank K. Easterling for stimulating this project.

References

1. J. Koo, B.V.N. Rao, G. Thomas, Metal Progress, 66, (1979).
2. E.W. Muller, J.A. Panitz, S.B. McLane, Rev. Scient. Instrum., 39, 83, (1968).
3. M.K. Miller, P.A. Beaven, R.J. Lewis, G.D.W. Smith, Surf. Sci., 70, 470, (1978).
4. J.Y. Koo, G. Thomas, Proc. of EMSA, Claitor's Publishing Division, Baton Rouge, LA, 118, (1975).
5. B.V.N. Rao, G. Thomas, Proc. Int. Conf. on Martensitic Transformations (ICOMAT) Cambridge, MA, 12, (1979).
6. R. Sinclair, G. Thomas, Met. Trans. A, 9, 373, (1978).
7. M.K. Miller, P.A. Beaven, G.D.W. Smith, Surface and Interface Analysis, 1 149, (1979).
8. Z. Nishiyama, Martensitic Transformations, Academic Press, London, 319, (1978).
9. G. Thomas, Met. Trans. A, 9, 439, (1978).

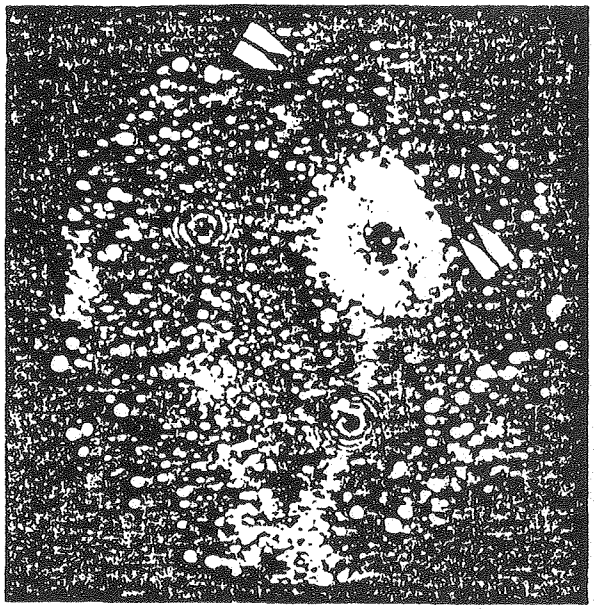

FIG 1

Neon Field Ion Micrograph of the martensite matrix (14.1 KV). Note the thin band of retained austenite (arrowed) and the spiral indicating a dislocation.

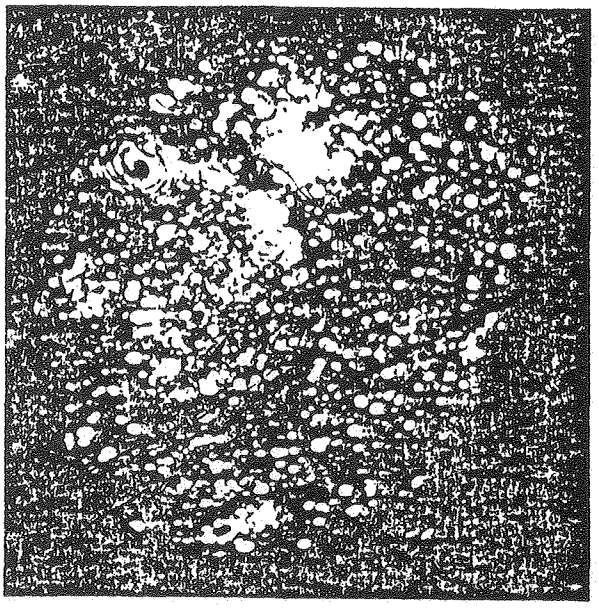

FIG 2

Neon Field Ion Micrograph of the same specimen as in fig.1 but later in the evaporation sequence (14.2 KV). The intersection of the austenite and specimen surface is now nearer the centre of the image.
Note the dislocation spiral. arrowed

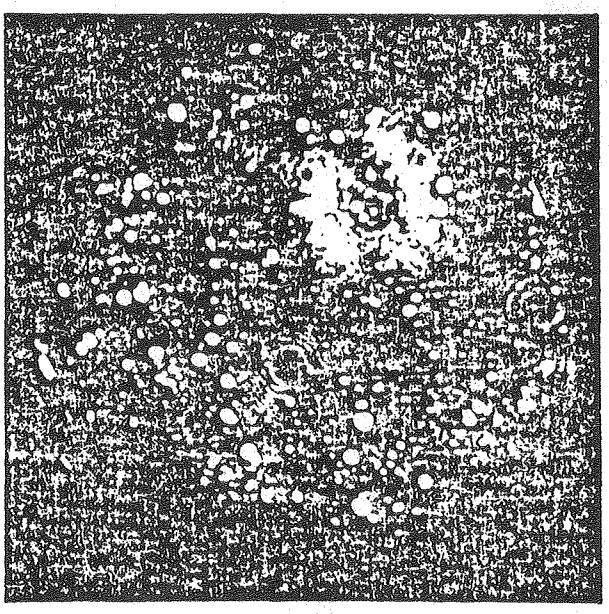

FIG 3

Neon Field Ion Micrograph of the martensite matrix of another specimen showing a carbide and a dislocation spiral (10.0 KV).

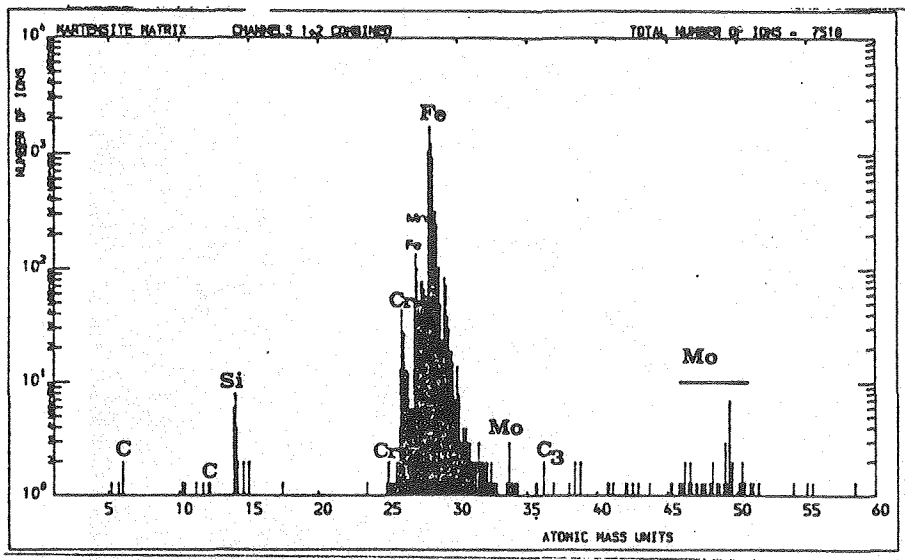

FIG 4

Typical mass spectrum of the martensite

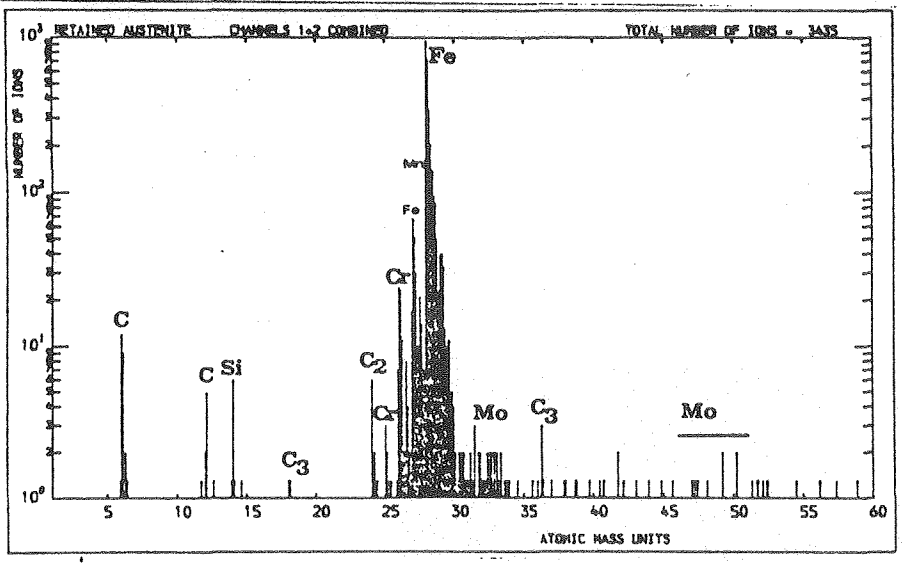

FIG 5

Typical mass spectrum of the retained austenite

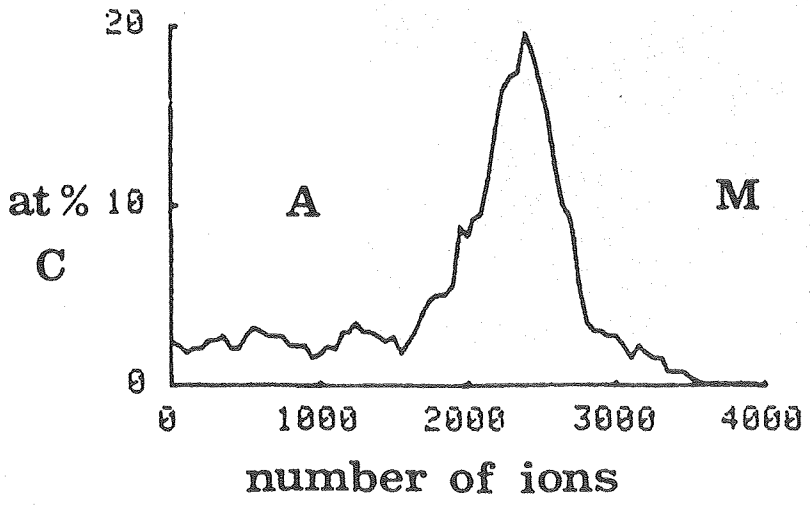

FIG 6

Distribution of carbon across the martensite-austenite interface